

# Influence of resin content and compaction pressure on the mechanical properties of SiC–Si composites with sub-micron SiC microstructures

Matthias Wilhelm \*, Silvia Werdenich, Werner Wruss

*Institute for Chemical Technology of Inorganic Materials, Vienna University of Technology, Austria*

Received 10 May 2000; accepted 10 September 2000

---

## Abstract

The influence of resin content (15–20, 25 wt.%) and compaction pressure (75, 100, 125 MPa) on the mechanical properties and microstructure of SiC–Si composites with sub-micron microstructure has been evaluated. To produce the composites three powders with particle sizes in the range of 0.22–0.70 µm were used. Before application the SiC powders were treated with hydrofluoric acid to remove the extent of SiO<sub>2</sub>. Due to this treatment a successful infiltration of green-bodies, even of those produced of SiC powder with a mean particle size of 0.22 µm, was possible. The fracture toughness and bending strength increased with increasing resin content. The highest value of strength was observed at 733 MPa for the composites produced of SiC powder with a mean grain size of 0.70 µm and a resin content of 25 wt.%. Within this composite the free silicon content was reduced to 12 vol.%. In regard to previous experiments this is a reduction of more than 50%. These results are a consequence of the lowering of the free silicon content of the composites when increasing the resin amount. With decreasing SiC starting particle size the mechanical properties decreased but they were independent on compaction pressure. © 2001 Elsevier Science Ltd. All rights reserved.

**Keywords:** Mechanical properties; Microstructure-final; Pressing; Reaction bonding; SiC

---

## 1. Introduction

Silicon-infiltrated silicon-carbide (SiSiC, SiC–Si, RB–SiC) is a well known material providing outstanding properties. This ceramic has particular advantages in terms of production and costs since such ceramic parts can be produced at relatively low temperatures (1500–1700°C) with no or less shrinkage so net-shape processing is possible. Due to its good resistance against oxidation and corrosion, excellent tribological properties and high mechanical strength up to 1300°C,<sup>1–4</sup> this ceramic is used in a number of different industrial applications, e.g. as a material for combustion chambers, gas-turbines, heat-exchangers, seal-rings, valve discs and ceramic engine parts.<sup>5–8</sup> It is well known that the main problem in using this ceramic is its brittleness.<sup>9</sup>

Many efforts have been undertaken to improve the mechanical properties of SiC–Si.

These ceramics are usually fabricated by infiltrating a porous compact consisting of α-silicon carbide (SiC) and carbon with liquid silicon (Si). It is well known<sup>10</sup> that one limiting factor to obtain Si–SiC ceramics of high strength is the amount of free silicon in the composites since the SiC:Si interfaces and the brittle free silicon phase are preferential paths for fracture.<sup>11</sup>

In order to reduce the amount of free silicon to obtain better mechanical properties SiC–Si composites made of two powders with different grain sizes (bimodal SiC structure) were produced in earlier investigations.<sup>12</sup> These composites contained low free silicon contents but their mean bending strength was limited at 350 MPa.

The following experiments with composites made of one SiC powder (monomodal SiC structure)<sup>9</sup> showed that using SiC powders with a mean grain size in the range of 3–12.8 µm a clear linear enhancement of the bending strength with decrease of original SiC size was

---

\* Tel.: +43-1-58801-16130; fax: +43-1-587-79-18.

E-mail address: mwilhelm@fbch.tuwien.ac.at (M. Wilhelm).

observed. However, a further reduction of the SiC particle size to 0.5 µm brought no increase of the mean bending strength. The authors assumed that four effects influence the mechanical properties of the composites. These are the oxygen content of the starting SiC powders, internal stresses, the density of pressing failures and the free silicon content.

In further investigations<sup>13</sup> the oxygen content of the powders used was decreased by etching with hydrofluoric acid. Due to eliminating the influence of SiO<sub>2</sub> on the infiltration of the green compacts a successful silicidation of green bodies especially of those produced of SiC powder with a mean grain size of 0.22 µm was possible.

In order to reduce the stresses within the SiC–Si microstructure, which are caused by the thermal expansion of silicon during cooling down,<sup>14,15</sup> the composites were annealed at 1000, 1100 and 1200°C, respectively.<sup>13</sup> It was noticed that the effects of internal stresses on the mechanical properties are very low and independent of annealing temperature. In Ref. 9 it was assumed that defects in the microstructure are a consequence of an imperfect technology. During the mixing step with the tumbling mixer a homogeneous distribution of the soot cannot be achieved so that carbon islands remain after compaction. An increased density of pressing defects, e.g. cracks filled with silicon, silicon islands, non-connected granulate grains after compaction, which mainly affect the mechanical properties of the specimens was observed within the composites made of submicron SiC powders. Furthermore, a low plasticity of the granulate grain as well as grain friction have a negative influence on the microstructure and therefore on the mechanical properties of the produced specimens.

Furthermore, it was observed that due to enhanced friction between the granulate and the pressing die the compaction was different in the middle and the edges of the samples. In Refs. 13 and 16 a negative effect of high amounts of free silicon on the bending strength was established. The high amount of free silicon phase as well as the small grain size of the original SiC powder used causes an increasing occurrence of SiC:Si interfaces which weaken the SiC–Si composite.<sup>13,16</sup> One possible way to reduce the amount of free silicon is the increase of the free carbon content of the green bodies.

The present work deals with the production of SiC–Si composites with sub-micron SiC grain structure. The grain size of the starting SiC is in the range of 0.22–0.70 µm. To eliminate the influence of SiO<sub>2</sub> on the infiltration of the green compacts the SiC powders used in this study shall be etched. To determine the influence of resin content on the amount of free silicon the resin content is varied in the range of 15–25 wt.%. In addition, the compaction pressure is varied (75–125 MPa) to reduce the frequency of pressing failures in the composites.

## 2. Experimental procedure

Three α-SiC powders (0.70, 0.51, 0.22 µm), carbon black, phenolformaldehyd resin (Perstorp AG, Sweden) an si-metal (Gesellschaft für Elektrometallurgie, Germany, mean Si grain size 0.2 µm) were used as starting materials. The SiC powders were provided by two suppliers, ESK, Kempten, Germany (0.70 µm SiC) and H.C. Starck, Waldshut-Tiengen, Germany (0.51 and 0.22 µm SiC).

Tables 1 and 2 show the typical characteristics of the Si and the SiC powders used.

The exact producing process has been described elsewhere.<sup>9,13</sup>

To reduce the extent of SiO<sub>2</sub> of the SiC powders used in this study the SiC powders were etched 24 h with 20 vol.% hydrofluoric acid. However, a low oxygen content (a thin SiO<sub>2</sub> layer) is necessary for a complete infiltration since the produced SiO reacts with the carbon near the surface and in that way opens surface-near pores.<sup>17</sup> Furthermore, it has to be assumed that an increased compaction pressure makes the penetration of silicon into the green compact more difficult. Therefore, a stop at 1300°C has been set in the infiltration programme. At this temperature the residual SiO<sub>2</sub> reacts partly with carbon and so gaseous CO is produced. This CO leaves the compact and in that way opens surface-near pores.

After the etching procedure the SiC powders (75, 80 or 85 wt.%, depending on the resin content) and the soot (5 wt.%) were suspended in acetone and homogenised for 24 h in a tumbling mixer. The organic binder (15–25 wt.% phenolformaldehyd resin) was then added and the acetone was removed by distillation in order to obtain a dry product. This powder mixture was sieved,

Table 1  
Chemical composition of the silicon used

Mean Si particle size [µm]	Purity (wt.%)
0.2	Si: > 99.7; Fe: 0.004; B: 0.003; Co: 0.008; Cr: 0.01; Cu: 0.015; Mo: 0.002; Ni: 0.02; Nb: 0.002; Ta: 0.002; V: 0.03; W: 0.003; Ti: 0.05; Sn: 0.003; Zn: 0.003

Table 2  
Characteristics of the SiC powders used

SiC-quality	Mean SiC particle size (µm)	Oxygen content (wt.%)	
		As supplied	After etching
RS-07	0.70	0.6	0.4
UF-15	0.51	1.7	0.7
UF-45	0.22	4.5	1.3

granulated and then dry pressed at 75, 100 or 125 MPa, respectively, to get green bodies.

The organic binder was hardened and cracked to carbon; for silicidation the contact infiltration technique was used. After cutting and polishing bars measuring  $40 \times 3 \times 4$  mm<sup>3</sup> were obtained.

The bulk density of the infiltrated samples was measured by Archimedes principle in water. The fracture toughness of the composites was determined using three point loading and single edge notched beam technique with a notch width of 100 µm, a span of 11 mm and a cross head speed of 1 mm/min (9 specimens for every material) at room temperature. The broken bars of this measurement were used to determine bending strength. The mean bending strength was measured on  $20 \times 3 \times 4$  mm<sup>3</sup> bars (18 specimens for every material) at room temperature using three point loading with a span of 11 mm and a cross head speed of 2 mm/min. For evaluation Weibull statistics was used.

### 3. Results and discussion

#### 3.1. Density

Tables 3 and 4 show the measured densities of the green compacts after compaction, hardening, cracking and infiltration. Fig. 1 (a)–(c) represents the dependence of green compact densities after compaction, hardening and cracking on the particle size of the used SiC. For this graph the results of the composites pressed at 100 MPa were used. The results of the specimens compacted at the other pressures (75 and 125 MPa, respectively) little differed from the plotted results. The calculation of

theoretical densities is described in Ref. 18. The volume fraction of free silicon within the composites can be estimated by an equation using theoretical densities of SiC (3.21 g/cm<sup>3</sup>) and Si (2.32 g/cm<sup>3</sup>).

The densities generally increased both with rising grain size of the SiC powders and with increasing resin content. That is to say, the increase of resin content in the green bodies proved a success since infiltrated densities up to 3.11 g/cm<sup>3</sup> have been obtained. After infiltration fully dense composites made of 0.70 and 0.51 µm powder were obtained (98–99% of theory). Due to the treatment of the powders with hydrofluoric acid also a successful infiltration of the composites produced of 0.22 µm SiC was possible, although the oxygen content was still relatively high (1.3 wt.%). The high oxygen content could be the reason for the remaining porosity within these composites (approximately 3%). The highest porosity (6%) was determined in the composite made of 0.22 µm SiC with 25 wt.% resin which was compacted at 125 MPa.

This observation can be explained by pressing failures which are caused by grain friction and occur more often within the composites made of ultrafine SiC qualities. Such defects are a consequence of sticking effects on the surface of the pressing mould. Furthermore, it has been found out that a higher resin content and an increasing compaction pressure, respectively, lead to difficulties in processing especially during the compaction.

#### 3.2. Free silicon content

The influence of SiC starting grain size, resin content and pressure on the free silicon content is described in Fig. 2 (a)–(c). The volume fraction of free silicon within

Table 3

Density values obtained after compaction, hardening, cracking and infiltration for composites made of RS–SiC powder

SiC-quality/ grain size (µm)	Resin content (wt.%)	Compaction pressure (MPa)	Density after compaction (g/cm <sup>3</sup> )	Density after hardening (g/cm <sup>3</sup> )	Density after cracking (g/cm <sup>3</sup> )	Density after infiltration (g/cm <sup>3</sup> )	Theoretical density (g/cm <sup>3</sup> )
RS-07 0.70	15	75	1.88 (61.6%)	1.81 (59.3%)	1.81 (59.3%)	$2.97 \pm 0.005$ (97.4±0.2%)	3.05 (100%)
			1.89 (62.0%)	1.82 (59.7%)	1.81 (59.3%)	$2.97 \pm 0.01$ (97.4±0.2%)	3.05 (100%)
			1.93 (63.1%)	1.87 (61.1%)	1.85 (60.5%)	$2.98 \pm 0.01$ (97.4±0.3%)	3.06 (100%)
		20	1.95 (64.1%)	1.87 (61.5%)	1.86 (61.2%)	$2.99 \pm 0.01$ (98.4±0.2%)	3.04 (100%)
	20	100	1.99 (65.2%)	1.91 (62.6%)	1.88 (61.6%)	$3.01 \pm 0.01$ (98.7±0.3%)	3.05 (100%)
			2.00 (65.6%)	1.92 (63.0%)	1.90 (62.3%)	$3.00 \pm 0.01$ (98.4±0.4%)	3.05 (100%)
			2.12 (67.5%)	2.03 (64.6%)	1.99 (63.4%)	$3.09 \pm 0.005$ (98.4±0.2%)	3.14 (100%)
		25	2.12 (67.5%)	2.03 (64.6%)	1.98 (63.1%)	$3.10 \pm 0.004$ (98.7±0.1%)	3.14 (100%)
	25	100	2.13 (67.8%)	2.04 (65.0%)	1.99 (63.4%)	$3.11 \pm 0.004$ (99.0±0.1%)	3.14 (100%)
			2.13 (67.8%)	2.04 (65.0%)	1.99 (63.4%)	$3.11 \pm 0.004$ (99.0±0.1%)	3.14 (100%)

the composites can be estimated by the equation using theoretical densities of SiC ( $3.21 \text{ g/cm}^3$ ) and Si ( $2.33 \text{ g/cm}^3$ ) e.g.  $V_{\text{Si}} = 3.648 - 1.136D$ , where  $D$  is the bulk density of the composites. Table 5 shows the measured contents of free silicon of the composites.

In general, the content of free silicon after the infiltration is influenced by the densities of the green compacts after cracking. That is to say, the higher the porosity of the composite the more volume can be taken up by silicon. Due to the increase of carbon content (resulted from cracked resin) more secondary SiC (from reacted liquid silicon with carbon) is produced which is growing into the existing porosity of the green-compact and, therefore, the free silicon content was reduced. Generally, the lowest volumes of silicon were obtained within the specimens produced of 0.70 and 0.51  $\mu\text{m}$  SiC, respectively; the highest within the composites made of 0.22  $\mu\text{m}$  SiC. This behaviour can be explained by reduced grain friction and sufficient compaction which lead to an almost ideal content of free silicon (12 vol %)

which was achieved using 0.70  $\mu\text{m}$  SiC and 25 wt.% resin compacted at 125 MPa. Compared to earlier studies<sup>9</sup> this is a decrease of the free silicon content up to 70%.

The volume of free silicon phase was reduced within the composites made of 0.22 SiC too, but the remaining free silicon content of approximately 30 vol.% is still rather high and can be explained by the low densities of these specimens. That means that these compacts contain more pores which are filled with liquid silicon during infiltration.

### 3.3. Microstructural analysis

Scanning electron micrographs of the polished surfaces of the composites showed homogeneous and very compact microstructures (Fig. 3). However, it was recognised that fractures originated from surface near defects such as silicon islands, microcracks or pores. Some of these defects are illustrated in Figs. 4 and 5.

Table 4

Density values obtained after compaction, hardening, cracking and infiltration for composites made of UF–SiC powders

SiC-quality/ grain size ( $\mu\text{m}$ )	Resin content (wt.%)	Compaction pressure (MPa)	Density after compaction ( $\text{g/cm}^3$ )	Density after hardening ( $\text{g/cm}^3$ )	Density after cracking ( $\text{g/cm}^3$ )	Density after infiltration ( $\text{g/cm}^3$ )	Theoretical density ( $\text{g/cm}^3$ )
UF-45 0.22	15	75	1.75 (59.7%)	1.68 (57.3%)	1.68 (57.3%)	2.89±0.01 (98.6±0.3%)	2.93 (100%)
			1.79 (60.9%)	1.72 (58.5%)	1.71 (58.2%)	2.88±0.01 (98.0±0.3%)	2.94 (100%)
			1.81 (61.6%)	1.73 (58.8%)	1.73 (58.8%)	2.89±0.01 (98.3±0.2%)	2.94 (100%)
		125	1.81 (61.6%)	1.73 (58.8%)	1.73 (58.8%)	2.89±0.01 (98.3±0.2%)	2.94 (100%)
	20	75	1.80 (60.6%)	1.71 (57.6%)	1.69 (56.9%)	2.90±0.004 (97.6±0.1%)	2.97 (100%)
		100	1.88 (62.9%)	1.79 (59.9%)	1.75 (58.5%)	2.93±0.02 (98.0±0.6%)	2.99 (100%)
		125	1.88 (62.9%)	1.78 (59.5%)	1.75 (58.5%)	2.94±0.01 (98.3±0.2%)	2.99 (100%)
	25	75	1.91 (63.0%)	1.79 (59.1%)	1.75 (57.8%)	2.95±0.01 (97.4±0.3%)	3.03 (100%)
		100	1.90 (62.7%)	1.78 (58.7%)	1.75 (57.8%)	2.95±0.01 (97.4±0.3%)	3.03 (100%)
		125	1.91 (62.8%)	1.80 (59.4%)	1.77 (58.2%)	2.87±0.03 (94.4±0.9%)	3.04 (100%)
		125	1.91 (62.8%)	1.80 (59.4%)	1.77 (58.2%)	2.87±0.03 (94.4±0.9%)	3.04 (100%)
UF-15 0.51	15	75	1.84 (62.2%)	1.78 (60.1%)	1.76 (59.5%)	2.94±0.01 (99.3±0.3%)	2.96 (100%)
			1.85 (62.3%)	1.79 (60.3%)	1.78 (59.9%)	2.95±0.01 (99.3±0.2%)	2.97 (100%)
			1.89 (63.4%)	1.82 (61.1%)	1.80 (60.4%)	2.95±0.005 (99.0±0.2%)	2.98 (100%)
		125	1.93 (63.7%)	1.85 (61.1%)	1.82 (60.6%)	2.99±0.005 (98.7±0.2%)	3.03 (100%)
	20	75	1.97 (64.6%)	1.89 (62.0%)	1.88 (61.6%)	2.99±0.005 (98.0±0.2%)	3.05 (100%)
		100	1.98 (64.9%)	1.90 (62.3%)	1.88 (61.6%)	3.01±0.01 (98.7±0.3%)	3.05 (100%)
		125	2.05 (65.9%)	1.96 (63.0%)	1.92 (61.7%)	3.08±0.01 (99.0±0.3%)	3.11 (100%)
	25	100	2.06 (66.2%)	1.96 (63.0%)	1.91 (61.4%)	3.08±0.004 (99.0±0.1%)	3.11 (100%)
		125	2.06 (66.2%)	1.96 (63.0%)	1.91 (61.4%)	3.08±0.004 (99.0±0.1%)	3.11 (100%)

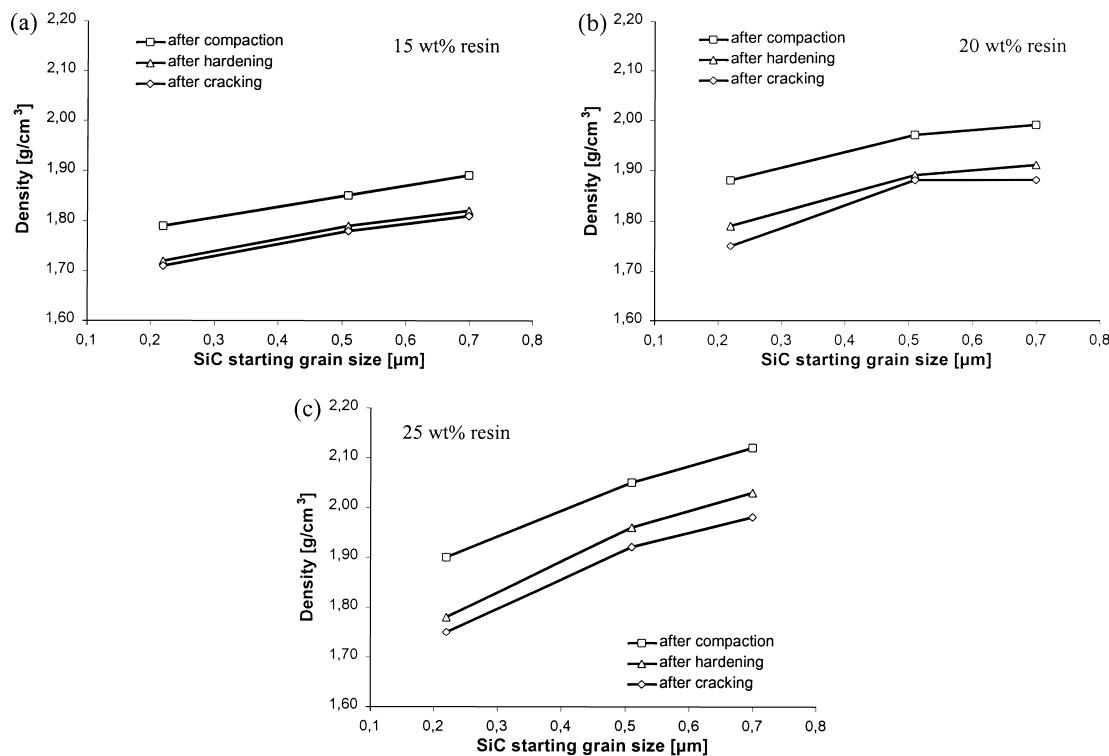


Fig. 1. Densities as a function of particle size of SiC powder compacted at 100 MPa and a resin content of (a) 15 wt.%, (c) 25 wt.% (data point sizes represent the standard deviation).

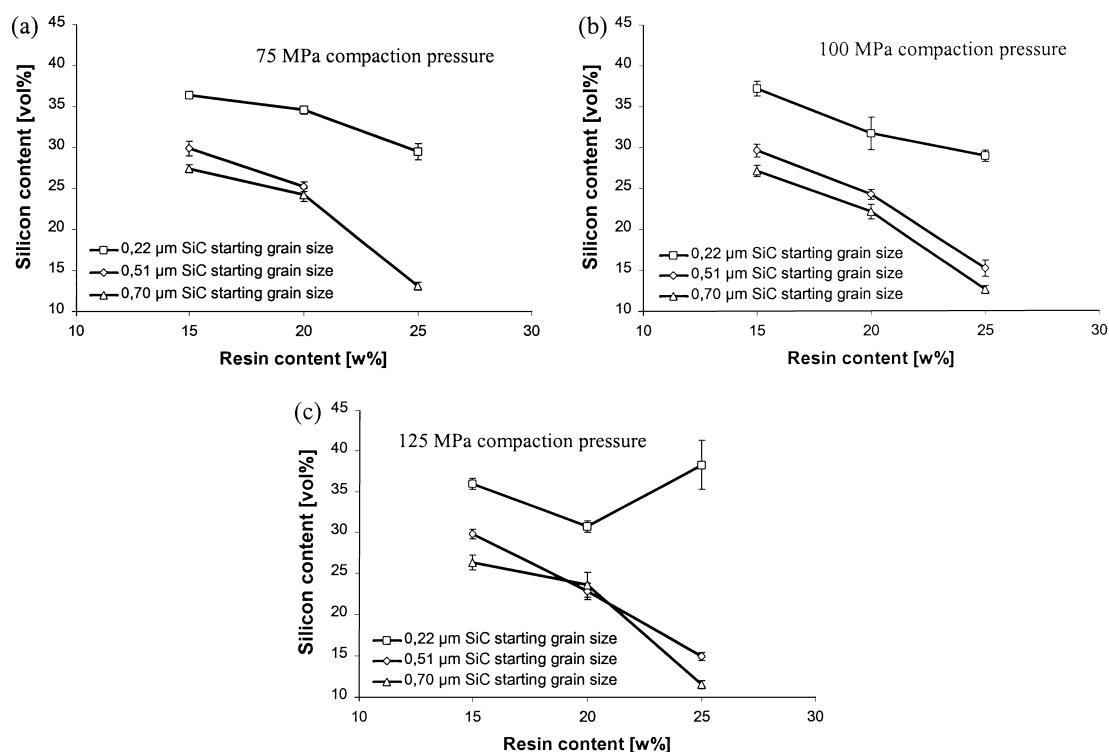


Fig. 2. Free silicon content as a function of resin content and particle size of SiC powder compacted at (a) 75 MPa, (b) 100 MPa, (c) 125 MPa.

Table 5

Free silicon content of the SiC–Si composites

SiC-quality/grain size ( $\mu\text{m}$ )	Resin content (wt.%)	Theoretical free silicon content (vol.%)			Free silicon content (vol.%)		
		Compaction pressure (MPa)			Compaction pressure (MPa)		
		75	100	125	75	100	125
UF-45 0.22	15	31.5	30.2	29.8	36.4±1.1	37.2±0.9	36.0±0.7
	20	27.5	24.8	24.8	34.6±0.5	31.7±2.0	30.7±0.7
	25	20.3	20.5	19.6	29.5±1.0	28.9±0.7	38.3±3.0
UF-15 0.51	15	27.6	26.7	25.7	29.9±0.9	29.6±0.8	29.8±0.6
	20	20.7	18.3	18.2	25.2±0.6	24.2±0.6	22.8±1.0
	25		11.3	11.7		15.2±1.0	14.9±0.5
RS-07 0.70	15	18.4	18.1	16.5	27.4±0.5	27.1±0.7	26.3±0.9
	20	19.3	18.4	17.5	24.2±0.8	22.1±0.9	23.6±1.5
	25	8.1	8.1	8.1	13.1±0.5	12.6±0.5	11.5±0.5

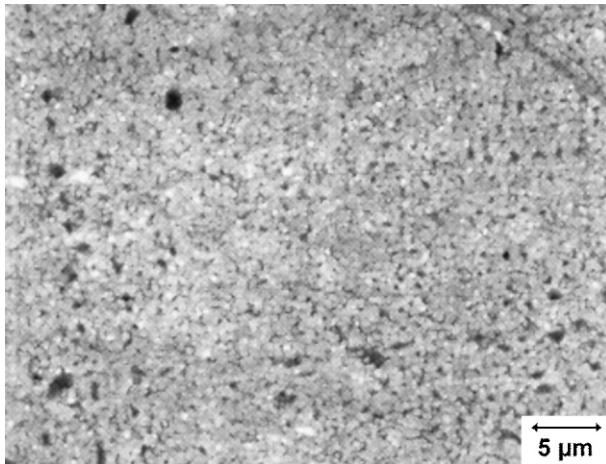


Fig. 3. SEM micrograph of the polished surface of the composite made of 0.22  $\mu\text{m}$  SiC (20 wt.% resin, 100 MPa) illustrating a homogeneous microstructure.

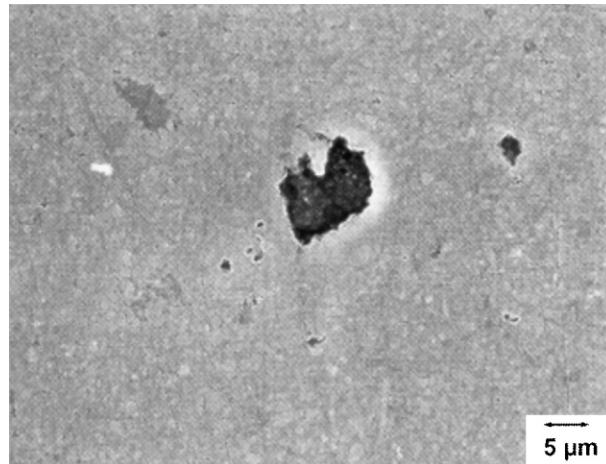


Fig. 5. SEM micrograph of the polished surface of the composite made of 0.70  $\mu\text{m}$  SiC (20 wt.% resin, 100 MPa) illustrating pores and a small silicon island.

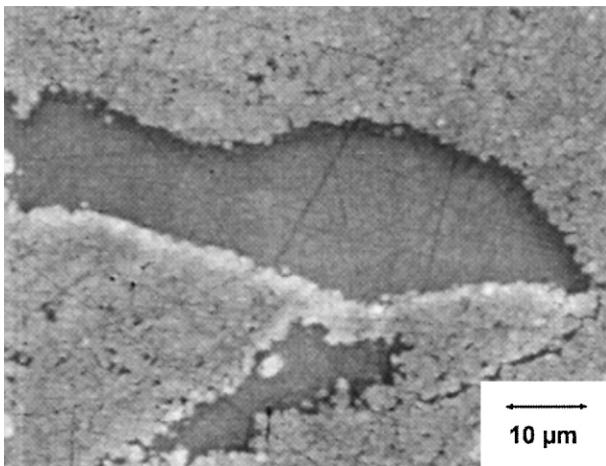


Fig. 4. SEM micrograph of the polished surface of the composite made of 0.51  $\mu\text{m}$  SiC (25 wt.% resin, 125 MPa) illustrating a silicon island.

In the microstructure of composites produced of 0.22  $\mu\text{m}$  SiC it was found that after compaction the original granulate grains sometimes were not completely combined and therefore the reaction area is not filled with liquid silicon. These defects can be explained by difficulties in processing, e.g. compaction, which lead to a high frequency of pressing failures. Further reasons are the low plasticity of the granulate during compaction and the high grain friction of the UF–SiC powders used. It is interesting to note that within the UF-composites sometimes big pores were found. In some of such pores needle shaped structures (with a length of 4–5  $\mu\text{m}$  and a diameter of 0.4  $\mu\text{m}$ ) were observed (Fig. 6). Using WDS-analysis these needles were determined to be SiC polycrystals. It was assumed that these structures result from a gaseous phase reaction of CO with silicon or SiO, respectively, during the infiltration process. These reactions seem to be possible since the silicidation is

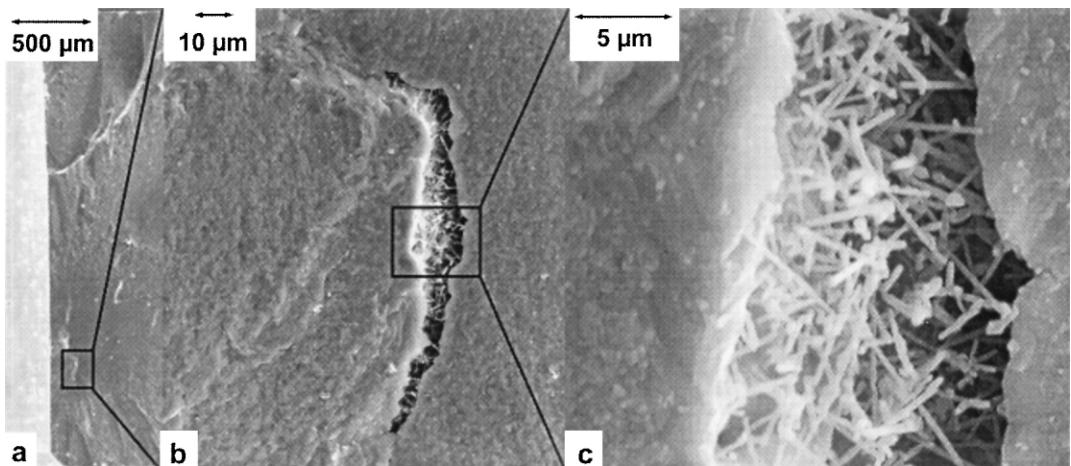


Fig. 6. SEM micrograph of the fractured surface of the composite made of 0.22  $\mu\text{m}$  SiC (75 MPa, 25 wt.% resin). (a) Survey. (b) The fracture originated from a crack. (c) Inside the crack needle shaped structures were found which were determined to be SiC polycrystals.

carried out at 1520°C in an isolated system. The required primary products originate from partial evaporation (Si) and from secondary reactions of carbon and silicon with  $\text{SiO}_2$  which is found on the surface of the SiC grains.

The microstructures of specimens made of 0.51  $\mu\text{m}$   $\alpha$ -SiC contained merely isolated silicon islands. Pores and silicon filled cracks were found more frequently. These defects result from problems during the compaction mainly at low compaction pressures as described before. During infiltration the arising porosity is filled up with silicon which is available in surplus. As well as in the specimens made of 0.22  $\mu\text{m}$  starting-SiC pores and cracks containing well crystallised SiC structures were found in these composites (Figs. 7 and 8). Comparing the size of these failures with the critical defect size which was calculated using the Griffith failure criterion,<sup>9</sup> it was assumed that fractures originated from these defects.

In the composites made of SiC with a starting grain size of 0.70  $\mu\text{m}$  such needle shaped structures were not found. If pores were observed, what merely happened in some cases, they were found in specimens where a compaction pressure of 75 MPa was used. In these samples fractures predominantly originated from silicon islands (Fig. 9). To some extent these defects included impurities (Fig. 10). EDS-analysis showed that these impurities consist of heavy metal silicides such as titanium or vanadium. It is well known<sup>11</sup> that fractures originate from such impurities. In addition, the high temperature behaviour of the SiC–Si composites is negatively influenced especially by low melting silicides. Furthermore, cracks filled up with silicon can be mentioned as fracture origins, too. In one composite a giant grain was spotted which possibly took its rise from inhomogeneities in the pressing process. Apart from that, the specimens produced of 0.70  $\mu\text{m}$   $\alpha$ -SiC showed a very homogeneous microstructure.

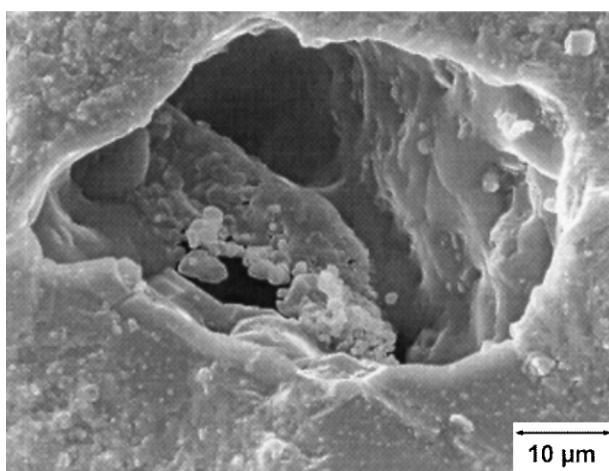


Fig. 7. SEM micrograph of the fractured surface of the composite made of 0.51  $\mu\text{m}$  SiC (15 wt.%, 75 MPa) illustrating a pore.

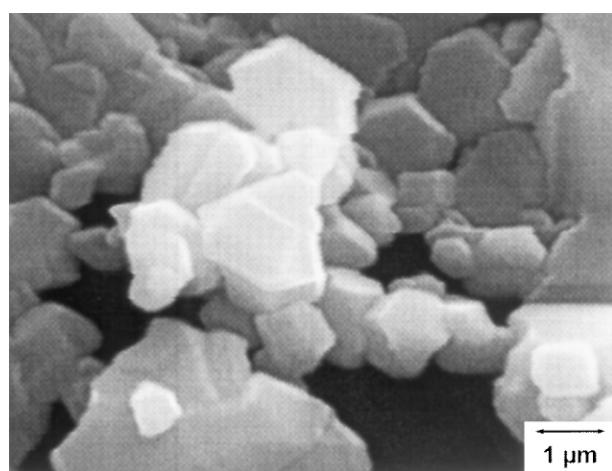


Fig. 8. Enlargement of the pore pictured in Fig. 7 illustrating crystals which were determined to be SiC polycrystals.

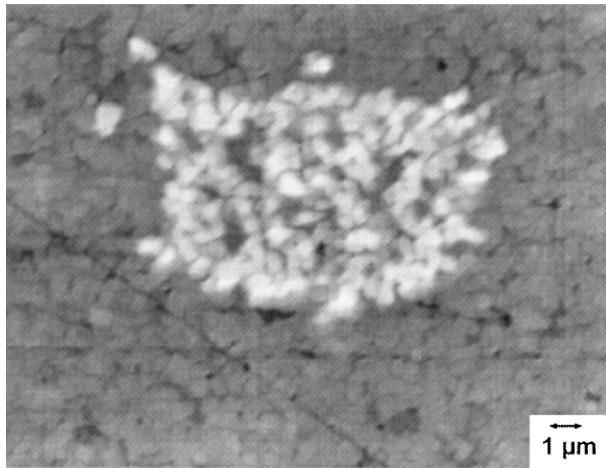


Fig. 9. SEM micrograph of the polished surface of the composite made of 0.70  $\mu\text{m}$  SiC (15 wt.% resin, 100 MPa) illustrating a silicon island containing impurities.

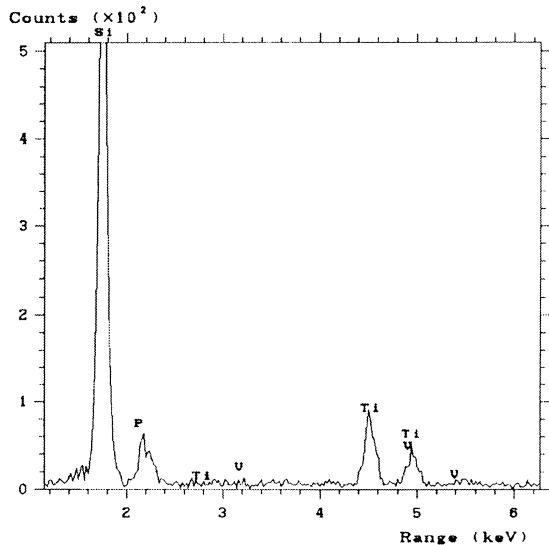


Fig. 10. EDS image of the impurities contained in the silicon island pictured in Fig. 9.

### 3.4. Mechanical properties

The mechanical properties of the composites are summarised in Table 6. The fracture toughness and mean bending strength are plotted as a function of the particle size of starting SiC, resin content and compaction pressure and are illustrated in Figs. 11(a)–(c) and 12 (a)–(c). Considering the standard deviation, the increase of resin content from 15 to 25 wt.% caused an enhancement in fracture toughness of approximately 20–25%. Due to a high frequency of pressing failures in the composites made of 0.22  $\mu\text{m}$  SiC these specimens showed the lowest  $K_{\text{Ic}}$ -values (from 2.4 MPa  $\sqrt{\text{m}}$  using 15 wt.% resin to 4.1 MPa  $\sqrt{\text{m}}$  using 25 wt.% resin, both at a compaction pressure of 75 MPa), the values of the composites produced of 0.51 and 0.70  $\mu\text{m}$  SiC powder were in the same range (from 3.3 MPa  $\sqrt{\text{m}}$  using the

UF–SiC quality with 15 wt.% resin and a pressure of 100 MPa to 5.4 MPa using the RS–SiC quality with 25 wt.% resin and a pressure of 75 MPa). The higher amount of free carbon caused an increasing content on secondary SiC and a reduction of the volume of free silicon phase in the SiC–Si structure, respectively. It is well known<sup>11,13,16</sup> that the weak parts in the SiC–Si microstructure are the SiC:Si interfaces as well as the free silicon itself. It is presumed that the decrease of free silicon content leads to an increase of fracture toughness. The maximum toughness value (5.4 MPa  $\sqrt{\text{m}}$ ) was obtained using 0.70  $\mu\text{m}$  SiC, 25 wt.% resin and a pressure of 100 MPa. The variation of pressure in the observed range (75–125 MPa) had just negligible influence on this mechanical property.

No general statement can be made for bending strength. The composites produced of SiC with a mean

Table 6  
Description of the mechanical properties of the SiC–Si composites

SiC-quality/grain size ( $\mu\text{m}$ )	Resin content (wt.%)	Fracture toughness (MPa $\sqrt{\text{m}}$ )			Mean bending strength (MPa)		
		Compaction pressure (MPa)			Compaction pressure (MPa)		
		75	100	12	75	100	125
UF-45 0.22	15	2.4±0.3	2.6±0.4	2.7±0.2	355±87	460±126	409±80
	20	3.3±0.8	3.1±0.2	3.9±0.7	457±92	483±89	497±71
	25	4.1±1.0	3.8±0.4	2.9±0.4	319±49	339±40	335±40
UF-15 0.51	15	3.4±0.4	3.3±0.3	3.6±0.4	465±94	526±108	492±82
	20	4.3±0.4	4.1±0.2	4.6±0.4	646±65	447±103	358±77
	25			4.1±0.8	4.5±0.8	291±29	462±61
RS-07 0.70	15	4.1±0.4	4.0±0.4	3.9±0.3	482±89	435±120	655±128
	20	4.5±0.6	3.9±0.4	3.7±0.3	489±77	653±114	538±126
	25	5.1±0.9	5.4±0.6	3.9±0.5	422±40	518±39	733±39

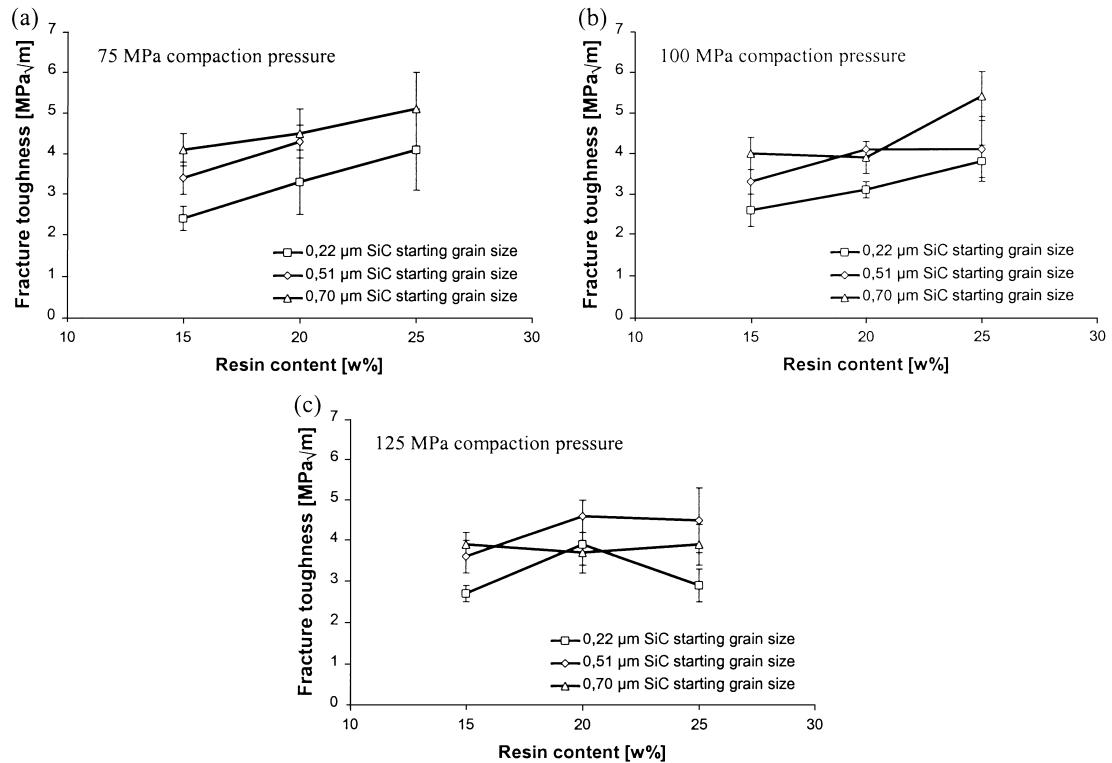


Fig. 11. Fracture toughness as a function of resin content and particle size of SiC powder compacted at (a) 75 MPa, (b) 100 MPa, (c) 125 MPa.

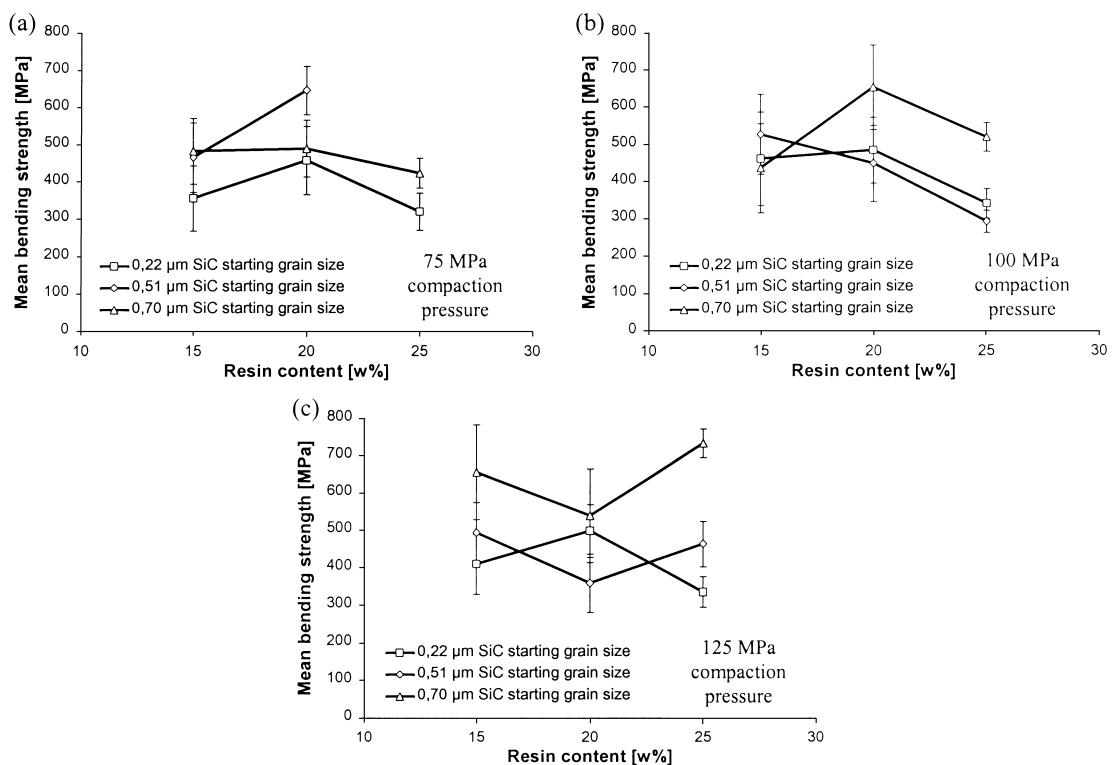


Fig. 12. Mean bending strength as a function of resin content and particle size of SiC powder compacted at (a) 75 MPa, (b) 100 MPa, (c) 125 MPa.

particle size of 0.22 µm showed the lowest  $\sigma_{B50}$ -values which were independent on resin content and compaction pressure, respectively. Within the composites made of 0.51 µm SiC powder the mean bending strength of the specimens compacted at 75 MPa increased with increasing resin content to a maximum value of 646 MPa. Further increase of the compaction pressure led to no improvement of strength. For the compacts with a SiC starting grain size of 0.70 µm no influence of resin content on bending strength could be recognised. However, an improvement of this composite property was reached by increasing the compaction pressure. The maximum  $\sigma_{B50}$ -value (733 MPa) was obtained for the specimen with 25 wt.% resin and 125 MPa pressure.

#### 4. Conclusions

In this study three commercial  $\alpha$ -SiC powders with a starting grain size in the range of 0.22–0.70 µm were used to produce SiC–Si composites with submicron SiC microstructure. The influence of resin content and compaction pressure on the mechanical properties as well as on microstructure was investigated:

1. Due to the treatment of the used SiC powders with hydrofluoric acid the extent of  $\text{SiO}_2$  was removed so that a successful infiltration of the green compacts, especially of those produced of SiC with a starting grain size of 0.22 µm, was possible.
2. Variation of the compaction pressure (75–125 MPa) had no significant influence on the mechanical properties or the microstructure of the composites. However, the higher pressures entailed difficulties in processing.
3. The mechanical properties of SiC–Si composites considerably depend on failures in processing which originate from inhomogeneous distribution of the granulate, enhanced SiC grain friction, humidity of the granulate and pressing failures (silicon islands, pores, ...), respectively.
4. An important quantity seems to be the resin content which was varied from 15 to 25 wt.% which as a consequence led to a higher amount of carbon. On the one hand, improvements in the properties of this cermet were achieved by increasing the resin content, e.g. a higher density (3.11 g/cm<sup>3</sup> after infiltration), a nearly ideal content of free silicon (12 vol.%) and an enhancement in fracture toughness to 5.4 MPa  $\sqrt{m}$  and in bending strength to 733 MPa, respectively. On the other hand, the more resin is used for producing the compacts the more difficult becomes the processing. That is to say, the resin content has to be optimised in future studies.
5. A homogeneous and compact microstructure was observed in most specimens. Further investiga-

tions gave rise to the assumption that fractures in nearly all cases originated from defects near the surface such as silicon islands, microcracks or pores.

#### Acknowledgements

We greatly acknowledge the support of this work by the “Jubiläumsfonds der sterreichischen Nationalbank”, project No. P6281.

#### References

1. Willerment, P. A., Pettand, R. A. and Whalen, J. J., Development and processing of injection-moldable reaction-sintered SiC compositions. *Am. Ceram. Soc.*, 1978, **57**, 744–747.
2. John B. Wachtman. J. Structural ceramics, Vol. 29
3. Lim, C. and Iseki, T., Transport of fine-grained  $\beta$ -SiC in SiC/liquid Si system. *Adv. Ceram. Mat.*, 1988, **3**, 291–293.
4. Krauth et al., Ingenieurkeramische Bauteile für Anwendungen in der Energietechnik, Verfahrenstechnik, Metallurgie und Motorenbau, Keramische Komponenten für Fahrzeug-Gasturbinen III, 647ff. Springer Verlag, 1984.
5. Wei, G. and Tennery, V., Evaluation of tubular ceramic heat exchanger materials in residual oil combustion environment. ORNL/TM-757, March, 1981.
6. Popper., P., The preparation of dense self-bonded silicon carbide. In *Special Ceramics*. Heywood, 1969, pp. 209–219.
7. Sawyer, G. R. and Page, T. F., Microstructural characterization of REFEL (reaction-bonded) silicon carbides. *J. Mat. Sci.*, 1978, **13**, 885–904.
8. Trantina, G., Design techniques for ceramics in fusion reactors. *Nucl. Eng. Des.*, 1979, **54**(1), 676–677.
9. Wilhelm, M., Kornfeld, M. and Wruss, W., Development of SiC–Si composites with fine-grained SiC microstructures. *J. Eur. Ceram. Soc.*, 1999, **19**, 2155–2163.
10. Chakrabati, O., Ghosh, S. and Mukerji, J., Influence of grain size, free silicon content and temperature on the strength and toughness of reaction-bonded silicon carbide. *Ceramics International*, 1994, **20**, 283–286.
11. Ness, J. N. and Page, T. F., Microstructural evolution in reaction bonded silicon carbide. *J. Mater. Sci.*, 1986, **21**, 1377–1397.
12. Blecha, M., Schmid, W., Krauth, A. and Wruss, W., Herstellung grobkörniger, auf hohen SiC-Gehalt optimierter SiC-C-Grünkörper für die Herstellung von SiSiC. *Sprechsaal*, 1990, **123**(3), 263–268.
13. Wilhelm, M. and Wruss, W., Influence of annealing on the mechanical properties of SiC–Si composites with sub-micron SiC microstructures. *J. Eur. Ceram. Soc.*, 2000, **20**, 1205–1213.
14. Gmelins Handbuch der anorganischen Chemie, Teil 15 B (Silizium), Verlag Chemie, 1959, pp. 63–65.
15. Cohrt, H., Herstellung, Eigenschaften und Anwendung von reaktionsgebundenen siliziuminfiltriertem Siliziumcarbid. *Werkstofftechnik*, 1985, **16**, 277–285.
16. Yang, J.H., Han, I.S., Woo, S.K., Cho, K. and Suhr, D.S., Fabrication and characterization of reaction bonded silicon carbide and reaction bonded silicon carbide / molybdenum disilicide composite. In: Yen, D. and Fu, X. (Ed.), *Int. Symp. Ceram. Mater. Compos. Engines*, 5th Meeting. World Scientific, Singapore.
17. Forrest, C., Kennedy, P. and Shennan, J., The fabrication and properties of self-bonded silicon carbide, TRG Report 2053 (S), 1970.
18. Forrest, C., Kennedy, P. and Shennan, J., The fabrication and properties of self-bonded silicon carbide. *Special Ceramics*, 1972, **5**, 99–123.